

Line Broadening and Decoherence of Electron Spins in Phosphorus-Doped Silicon Due to Environmental ^{29}Si Nuclear Spins

Eisuke Abe,¹ Akira Fujimoto,² Junichi Isoya,³ Satoshi Yamasaki,⁴ and Kohei M. Itoh^{1,2},

¹ Department of Applied Physics and Physico-Informatics,
Keio University, 3-14-1 Hiyoshi, Yokohama 223-8522, Japan

² CREST, Japan Science and Technology Agency, 4-1-8 Honcho, Kawaguchi, 332-0012

³ Research Center for Knowledge Communities, University of Tsukuba, 1-2 Kasuga, Tsukuba City 305-8550, Japan

⁴ Diamond Research Center, National Institute of Advanced Industrial Science and Technology,
Tsukuba Central 2, 1-1-1 Umezono, Tsukuba City 305-8568, Japan

(Dated: March 23, 2024)

Phosphorus-doped silicon single crystals with 0.19 % f ^{29}Si 99.2 %, where f is the concentration of ^{29}Si isotopes, are measured at 8 K using a pulsed electron spin resonance technique, thereby the effect of environmental ^{29}Si nuclear spins on the donor electron spin is systematically studied. The linewidth as a function of f shows a good agreement with theoretical analysis. We also report the phase memory time T_M of the donor electron spin dependent on both f and the crystal axis relative to the external magnetic field.

PACS numbers: 03.67.Lx, 28.60.+s, 76.30.-v, 76.60.Lz

Electron spin resonance (ESR) in phosphorus-doped silicon (SiP) at low temperatures is now a textbook example of how an electron spin in a solid interacts with nuclei. In this system, the donor ^{31}P nucleus, the electron bound to it, and ^{29}Si nuclei randomly occupying $f = 4.7\%$ of the lattice sites of natural Si, all carry the smallest possible spin angular momentum $\sim 1/2$. The ESR spectrum exhibits a doublet separated by 4.2 mT due to the contact hyperfine (hf) interaction with ^{31}P . In addition, the electron is subject to the hf field from ^{29}Si nuclei, since the orbital part of the electron wavefunction spreads over thousands of lattice sites. It was soon realized that this interaction inhomogeneously broadens the ESR lines. A ^{29}Si nucleus at the i th site shifts the precession frequency of the electron spin by $a_i/2$, according to the direction of the nuclear spin. a_i is the isotropic hf constant at the i th site. As long as the number of the electron spins participating in the ESR line is large and the total amount of the hf field each electron spin feels is stochastic, the resultant line shape will be approximated by the Gaussian distribution, for which the FWHM linewidth B_e and the root-mean-square linewidth B_{rms} are related by

$$B_e = 2 \sqrt{\frac{p}{2 \ln 2}} B_{rms}; \quad (1)$$

B_{rms} is written, neglecting the polarization of ^{29}Si nuclear spins, as [1]

$$B_{rms} = \frac{h}{2\pi} \sqrt{\sum_{i=1}^N \frac{a_i^2}{4}}; \quad (2)$$

where a_i is rescaled in the unit of tesla, and the sum runs over all the sites but the origin. Electron-nuclear double resonance (ENDOR) has allowed the experimental determination of a_i at a number of sites, and a good agreement was found between the linewidth in natural Si and the

one deduced from Eq. (2) [2]. However, neither is obvious, when f is reduced, if the square root dependence on f still holds nor the line remains Gaussian. This is one of the subjects we will verify in this contribution.

The inhomogeneous line broadening is a consequence of static shifts of the electron spin precession frequencies. In reality, ^{29}Si nuclei which caused the shift are mutually coupled through the magnetic dipolar interactions. Hence the nuclei are also able to cause a temporal change of the electron spin precession frequency by flipping their spins. This leads to decoherence of the electron spins due to spectral diffusion [3], which has gained revived attention in connection with spin-based quantum computing. It is suggested that decoherence due to nuclear-induced spectral diffusion could be an ultimate bottleneck for quantum computing schemes based on GaAs quantum dots (QDs) [4, 5, 6]. In this context, SiP is a promising testbed for studying nuclear-induced spectral diffusion, not only because quantum computers based on SiP have been proposed [7], but also because the concentration of environmental nuclei is controllable, which is impossible in III-V compounds whose available isotopes all possess non-zero nuclear spins.

In this contribution, we experimentally study inhomogeneous line broadening and nuclear-induced decoherence of the P donor electron spins in isotopically controlled Si single crystals whose ^{29}Si concentrations f range from 0.19 % to 99.2 %. Isotopically purified Si is now in wide use for the study of isotope effects in Si [8], and preparations of the samples with controlled f (such as 50 %) were accomplished in the following manner: First, two bars of isotopically purified ^{29}Si or ^{28}Si and natural Si were set together, and partially melted into one by optical heating. The mass ratio of the two bars were chosen to achieve desired f . The combined bar was made single-crystal by the coating zone (Fz) method using another

TABLE I: Summary of isotopically controlled Si single crystals. The ^{29}Si concentration f [%], crystal growth method (Czochralski or floating zone), net donor concentration N_d [10^{15} cm^{-3}], spin-lattice relaxation time T_1 [ms], FWHM of the ESR lines B_e [mT], and $R = M_4/3(M_2)^2$, obtained from experiments (R_{exp}) and simulations (R_{sim}), are listed.

Sample	f^a	Cz/Fz ^b	N_d^c	T_1	B_e	R_{exp}	R_{sim}
^{29}Si -0.2% ^d	0.19	Cz	0.3	11.0	0.023	1.9	f
^{29}Si -0.3%	0.31	Fz	0.6	13.1	0.082	1.7	f
^{29}Si -1%	1.2	Fz	0.7	10.0	0.078	1.6	1.65
^{29}Si -5% ^e	4.7	Cz	0.8	15.8	0.26	1.0	1.15
^{29}Si -10%	10.3	Fz	1.6	14.6	0.42	1.0	1.06
^{29}Si -50%	47.9	Fz	0.6	14.9	0.89	1.0	1.00
^{29}Si -100% ^{de}	99.2	Cz	0.8	4.4	1.22	1.1	0.98

^aDetermined by secondary ion mass spectroscopy (SIMS).

^bCrystal growth by the Fz method was carried out with the same apparatus as used in Ref. 9.

^cDetermined from the temperature dependent Hall effect measured by the van der Pauw method (down to about 20 K). Residual acceptor concentrations are of the order of 10^{13} – 10^{14} cm^{-3} .

^dFurther information is found in Ref. 10. ^{29}Si -0.2% here corresponds to isotopically purified ^{30}Si in the reference.

^eThe same samples as used in our previous work (Ref. 11).

^fThe simulations exhibit significant counts at the origin (no nuclei are found in any of the 176 sites), and R is not calculated.

bar of natural Si as a seed crystal. All the procedures were carried out in high purity argon gas atmosphere. Care was taken to achieve uniform distribution of ^{29}Si atoms. Finally, the single crystals of about 5 mm in diameter and a few centimeters in length were grown along [001]. Information on the samples used in this work is summarized in Table I. The net donor concentrations N_d were controlled to 10^{15} cm^{-3} to minimize unwanted dipolar interactions among the donor electron spins, but still ensuring the measurement sensitivity.

Pulsed ESR experiments were carried out using a Bruker Elexsys E580 spectrometer equipped with an Oxford ER 4118 CF cryostat. We exclusively applied a Hahn echo sequence given by $\pi/2 - \tau - \pi - \text{Echo}$, where τ is the interpulse delay and the duration of the $\pi/2$ pulse was set to 16 ns. The measurement temperature must be chosen properly [11]: It has to be below 10 K for the study of spectral diffusion, otherwise the phase memory time T_M is dominated by the spin-lattice relaxation time T_1 due to an Orbach process [12, 13]. On the other hand, at temperatures below 4 K, extremely long T_1 reduces the efficiency of our pulsed experiments in which each echo sequence needs to be repeated at a time interval much longer than T_1 . We found 8 K to be optimal: low enough for T_M not to be limited by T_1 but high enough to ensure a reasonable measuring time. T_1 listed in the fifth column of Table I, measured by an inversion recovery method, vary with samples, but show no marked correlations with f nor N_d . We presume that this difference in T_1 has little effect on the difference in T_M , as long as T_1 of one sample is much longer than its T_M . The repetition

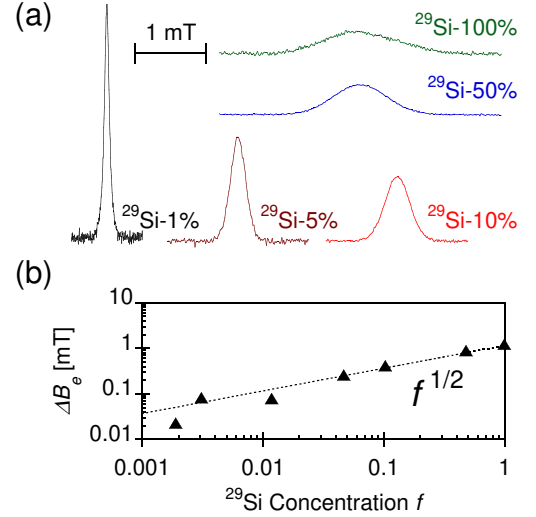


FIG. 1: (Color online) (a) Echo-detected ESR spectra of SiP. Only the normalized high-field lines are shown. The horizontal (magnetic field) and vertical (echo intensity) axes are arbitrarily shifted, and the small background signals are subtracted for clarity. (b) FWHM linewidth B_e as a function of f . The dotted line is a theoretical prediction, as explained in the text.

rate of the Hahn echo sequence was then set to 80 ms.

The echo-detected ESR spectra were obtained by measuring the intensity of the Hahn echo as a function of the external magnetic field B_0 with fixed τ . The high-field lines of the doublets are shown in Fig. 1-(a). The lines are Gaussian in $f = 4.7\%$, while in $f = 1.2\%$ the lines resembled Lorentzian (shown only for ^{29}Si -1%). The same features were confirmed from the low-field lines (not shown). Comparison between experimental linewidths and those deduced from Eqs. (1) and (2) is straightforward. Hale and Meier have determined a_1 for 176 lattice sites through ENDOR [14], and we will use the values reported in Table II of Ref. 14, dividing them by $g_B \mu_B \hbar$. Figure 1-(b) plots both theoretical and experimental B_e as a function of f , which agree quite satisfactorily. B_e at $f = 99.2\%$ is calculated to be 1.15 mT, which accounts for 94% of the experimental value, 1.22 mT. The underestimation of 6% is acceptable, since we included only 176 sites. The rest of thousands of sites will have very small isotropic hf constants, and increase the linewidth further, but not largely. This result, together with the fact that the linewidths are independent of the crystal orientations within experimental errors, justifies the exclusion of the anisotropic term of the hf interaction.

The line shapes in $f = 1.2\%$ are no longer Gaussian, and the use of Eq. (1) is dubious. A general method to characterize a line shape is to calculate the quantity R defined as $M_4/3(M_2)^2$, where M_2 and M_4 are the second and fourth moments of the line [15]. A Gaussian curve has R of unity. On the other hand, R for a pure Lorentzian curve cannot be defined, since both M_2 and

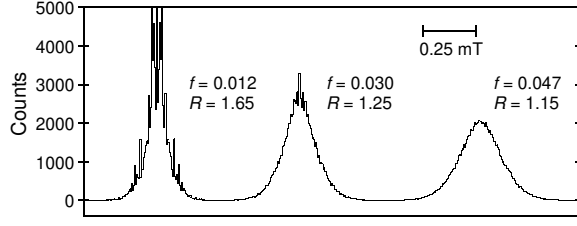


FIG. 2: Simulations of the ESR lines of SiP for $f = 1.2\%$, 3.0% , and 4.7% . The total counts for each line is 10^5 , and the width of each bar is set to 0.005 mT. The horizontal (magnetic field) axes are arbitrarily shifted.

M_4 diverge. Hence R is a convenient measure to quantify the deviation from Gaussian. In the seventh column of Table I, R numerically calculated from the experimental lines are given. We set moderate cut-offs to exclude the contribution from signals remote from the line centers [15]. R deviates from unity for $f = 1.2\%$, and $R = 1.6 - 1.9$ is consistent with the previous report by Feher in isotopically purified ^{28}Si of 99.88% ($R = 1.8$ is given in Table V of Ref. 2). The reason for this change to happen may be explained as follows: When f is reduced, it becomes rare to encounter ^{29}Si nuclei near the donor, where a_1 can be larger than the observed B_e [16]. Once such a ^{29}Si nucleus having a large a_1 is found, the electron spin is kicked out from the center part of the line, and there is no chance of its returning to the center, since other ^{29}Si nuclei are likely to have small a_1 . Those electron spins can only contribute to form wings of the line. This qualitative argument can be checked by a simple simulation, in which the known 176 sites are assumed to be occupied, independently with probability f , by ^{29}Si nuclei which are up or down with probability one-half. Then the hf shift of an electron spin is computed. Repeating the procedure 10^5 times, a frequency histogram should portray the observed line. The eighth column of Table I lists R calculated from each simulated line, and Fig. 2 shows simulated lines for $f = 1.2\%$, 3.0% , and 4.7% . It is seen that R gradually increases as reducing f , and deviates from unity. The agreement between R_{exp} and R_{sim} for $f = 1.2\%$ is good, even though the histogram is strongly peaked at the origin due to the limited number of the sites considered. It is interesting to continue this work to lower- f samples in order to seek for the intrinsic linewidth, or the boundary at which other broadening mechanisms prevail [17].

Now we examine the echo decay behavior by changing B_0 was fixed at the centers of the high-field lines. We define T_M as the time at which the envelope of an echo decay curve damps to $1/e$ of its initial echo intensity. Figure 3 shows echo decay curves as a function of 2τ , when B_0 is along the [001] crystal axis. The strong oscillation observed in the high- f samples is electron spin echo envelope modulation (ESEEM). Since this effect has already been analyzed by us [11] and by Ferretti et al. [18], it will

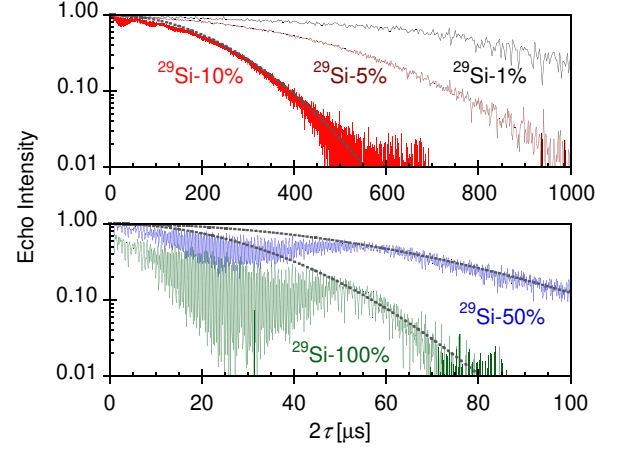


FIG. 3: (Color) Hahn echo decay curves as a function of 2τ when B_0 is along the [001] crystal axis. Note that the scales of horizontal axes in upper and lower panels differ by an order of magnitude. Gaussian fits to the echo decay envelopes are superposed on the data of ^{29}Si -10%, 50%, and 100%. The oscillations due to ESEEM are also visible.

not be dealt in the present contribution.

For samples with $f = 4.7\%$, the echo decay envelopes are obscured by ESEEM. To deduce T_M , we approximate them as Gaussian of the form $\exp[-(2\tau/T_M)^2]$. To determine a more accurate form of the decay envelopes, which could contain several time constants of different origins, requires further research. We repeat the experiments as rotating the samples about the [110] axis to characterize the angular dependence of T_M . It takes maximum when $B_0 \parallel [001]$ and minimum when $B_0 \parallel [111]$ as shown in Fig. 4-(a). This result bridges a large gap of f in our previous report of T_M carried out when only ^{29}Si -100% and 5% were available [11]. T_M also exhibits a power-law-like dependence on f as shown in Fig. 4-(b). Empirical fittings suggest T_M / f with $\alpha = 0.86$ for $B_0 \parallel [001]$ and 0.89 for $B_0 \parallel [111]$. The ^{29}Si concentration dependence confirms that T_M is affected by the presence of ^{29}Si nuclei, and the angular dependence demonstrates that spectral diffusion plays a major role, since the tendency reflects the strength of the nuclear dipolar couplings. When $B_0 \parallel [111]$, one of the four tetrahedral bondings is parallel to B_0 , and this pair of nuclei gives rise to the strong dipolar coupling, which makes T_M shortest. When $B_0 \parallel [001]$, all the dipolar couplings between nearest neighbors vanish, so that T_M is longest.

The angular dependence of T_M in ^{29}Si -100% and 5% has been explicitly compared with theory developed by de Sousa and Das Sarma [4] in Fig. 1 of Ref. 19, showing reasonable agreement. There are other theories on nuclear-induced spectral diffusion, which are developed recently and applicable to SiP as well as GaS QDs [5, 6]. We believe our experimental results serve as a testbed for the validations of such theories.

The situation changes in $f = 1.2\%$. The forms of the

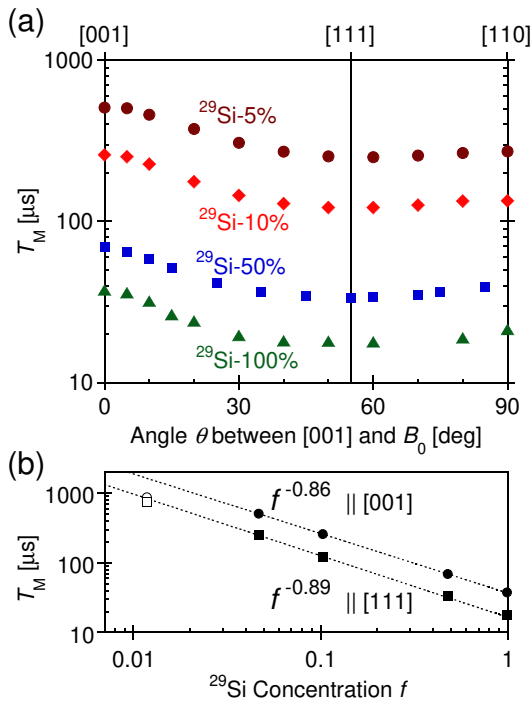


FIG. 4: (Color online) (a) Angular and (b) ^{29}Si concentration dependence of T_M . The circles (squares) in (b) represent T_M obtained when B_0 is along [001] (approximately [111]). Only the data points in the filled symbols are used for the fittings.

echo decay curves are quite dissimilar to Gaussian. The fittings by a single time constant are difficult, and T_M as the $1/e$ decay points are plotted in Fig. 4-(b). T_M of ^{29}Si -1% when B_0 is along [111] roughly coincides with the value extrapolated from the empirical power law. It must be noted that we encountered phase fluctuations of the quadrature-detected echo signals, occurring at 2 μs longer than about 500 μs , which significantly distorted the echo decay curves. This means, in effect, all the echoes are generated along one predetermined direction of the rotating frame, but each echo is detected along a random direction. A very similar instrumental problem has also been reported by Tyryshkin et al. when they measured purified ^{28}Si ($f = 0.08\%$, $N_d = 10^{15} \text{ cm}^{-3}$) [13]. Since our apparatus is of the same design as theirs, we suspect the two problems arise from the same origin [20]. Apart from this problem, it is not surprising that decoherence mechanisms other than spectral diffusion, such as the dipolar interactions among the electron spins and the T_1 effect, both of which we have assumed to minimize, come into play when f is reduced [13, 18]. Indeed, if we extrapolate the power law to $f < 1\%$, T_M will soon be comparable with T_1 at this temperature. Ultimately, the temperature and donor concentration dependence of T_M will have to be examined in detail to fully characterize the decoherence in this realm of f , which is beyond the scope of the present contribution. Our aim here is to investigate the decoherence dominated by nuclear-induced

spectral diffusion at fixed temperature and donor concentration.

In conclusion, we prepared isotopically controlled Si single crystals, and investigated the widths of the ESR lines and T_M of the donor electron spin as a function of the ^{29}Si concentration f (0.19 % $\leq f \leq 99.2\%$) at 8 K. We confirmed the square root dependence of the linewidth in $f = 4.7\%$, and also analyzed the deviation seen in $f = 1.2\%$. It is found that T_M is proportional to the power of f in $f = 4.7\%$, while further research is necessary in $f = 1.2\%$. We believe our results on T_M serve as a testbed for the validations of theories dealing with nuclear-induced spectral diffusion, and will provide insight into other systems such as electron spins confined in QD nanostructures.

We thank H.-J. Pohl for the purified ^{29}Si source, and A. Takano of NTT-AT for SIMS measurements of several samples. We also thank T. D. Ladd, S. A. Lyon, and A. M. Tyryshkin for fruitful discussions. E. A. was supported by Japan Society for the Promotion of Science. This work was partly supported by the Grant-in-Aid for Scientific Research in a Priority Area "Semiconductor Nanospintronics" (No.14076215).

Electronic address: kitoh@appliance.ac.jp

- [1] W. Kohn, in Solid State Physics (Academic Press, New York, 1957), vol. 5, p. 257.
- [2] G. Feher, Phys. Rev. 114, 1219 (1959).
- [3] B. Herzog and E. L. Hahn, Phys. Rev. 103, 148 (1956).
- [4] R. de Sousa and S. Das Sarma, Phys. Rev. B 68, 115322 (2003).
- [5] W. M. Witzel, R. de Sousa, and S. Das Sarma, Phys. Rev. B 72, 161306(R) (2005).
- [6] W. Yao, R.-B. Liu, and L. J. Sham, cond-mat/0508441.
- [7] B. E. Kane, Nature (London) 393, 133 (1998).
- [8] M. Cardona and M. L. W. Thewalt, Rev. Mod. Phys. 77, 1173 (2005).
- [9] K. Takyu, et al., Jpn. J. Appl. Phys. 38, L1493 (1999).
- [10] K. M. Itoh, et al., Jpn. J. Appl. Phys. 42, 6248 (2003).
- [11] E. Abe, K. M. Itoh, J. Isoya, and S. Yamasaki, Phys. Rev. B 70, 033204 (2004).
- [12] E. Yablonovitch, et al., Proc. IEEE 91, 761 (2003).
- [13] A. M. Tyryshkin, S. A. Lyon, A. V. Astashkin, and A. M. Raitsimring, Phys. Rev. B 68, 193207 (2003).
- [14] E. B. Hale and R. L. M. J. Phys. Rev. 184, 739 (1969).
- [15] A. Abragam, Principles of Nuclear Magnetism (Oxford University Press, 1960).
- [16] According to Ref. 14, a_1 is 0.21 mT at the (004) site and other 5 equivalent sites, and 0.16 mT at the (440) site and other 11 equivalent sites, and so forth.
- [17] The reason that the linewidth of ^{29}Si -0.3% is broader than that of ^{29}Si -1% is not clear. We have not confirmed the presence of nuclear species whose concentration is comparable with that of ^{29}Si (10^{20} cm^{-3}).
- [18] A. Ferretti, M. Fanciulli, A. Ponti, and A. Schweiger, Phys. Rev. B 72, 235201 (2005).
- [19] S. Das Sarma, R. de Sousa, X. Hu, and B. K. Coiller, Solid

State Commun. 133, 737 (2005).

[20] Tyryshkin et al. adopted magnitude detection to circumvent the phase problem [13], and could obtain a single

exponential echo decay, which was identified as due to instantaneous diffusion. The instantaneous diffusion is also studied in Ref. 18.